中國機械工程學刊第四十二卷第一期第 51~62 頁(民國一百一十年)
Journal of the Chinese Society of Mechanical Engineers, Vol.42, No.1, pp 51~62 (2021)

Vibrations of Rotating Ring Under Electric Field

Tao Yu*, Jiange Kou** and Yuh-Chung Hu***

Keywords: Electrostatics, initial stress, MEMS, vibratory ring gyroscope, rotating ring, rotor dynamics, vibration.

ABSTRACT

The vibration of rotating ring has got attention due to its wide application in engineering, such as vibratory ring gyroscope. This paper proposes an analytical model for the vibration of a rotating ring subjected to uniform electric field. The static pull-in voltage of a stationary ring is derived ahead the vibration analysis of the rotating ring. Then, a linearized electric-field model is derived and agrees well with the non-linear model when voltage lower than the static pull-in voltage. It is then applied on the analysis of the vibrations and dynamic stabilities of the rotating ring before static pull-in. The electric field will introduce an equivalent negative stiffness, which is proportional to the square of the voltage, into the rotating ring and thereby soften the ring and probably makes the vibration of the rotating ring unstable. The most interesting is that once the voltage enters the unstable region, one can further raise the rotational speed higher than the so-called critical speed to escape the unstable region. This is due to the initial stress induced by centrifugal force, which is proportional to the square of the rotational speed, makes the ring more rigid.

INTRODUCTION

The vibration of rotating ring has got much attention due to its broad application in engineering (Soedel, 2005), such as tires (Huang, 1987), bearing (Huang, 2013), compliant gears (Cooley, 2014), sensors (Kim, 2002), … and so on. The issues to be concerned in the vibration of ring includes the effects of rotatory inertia, foundation stiffness, pre-stress, rotation, and the forced vibration subjected to different loading types such as harmonic force, periodic force, distributed force, traveling load, …and so on. (Soedel, 2005, Huang, 1987, Beli, 2015, and Huang, 2014) Another example is the vibratory ring gyroscope, wherein the vibration of the ring is actuated and sensed by means of electrostatics. (Tao, 2011 and Esmaeili, 2006) It is an interaction between the structural vibration and electric field. Such electromechanical coupling problem has attracted attention in the last decade. (Chuang, 2010) The author, Hu, had studied the dynamic instability of a micro-beam subjected to the action of alternative electric field for the first time in 2004. (Hu, 2004) Since then, the dynamic instabilities of microstructures under electric field have been receiving much attentions continuously. Hu et al. had ever studied the forced vibration of a ring subjected to traveling electrostatic force. (Ye, 2012 and Li, 2014) Besides, the authors had published a paper for the first time to derive an analytical model for a rotating ring subjected to uniform electrical field. (Yu, 2018) However, that analytical model is applicable only in low rotational speed because of ignoring the initial stress induced by the rotational centrifugal force. Therefore, this paper is to modify that analytical model to be applicable on higher rotational speed by adding the initial stress induced by centrifugal force.

The feature size of thin-ring is its small ratio of thickness to radius, usually smaller than 0.1. (Beli, 2015) For example, the diameter of a vibratory ring gyroscope is about several hundred micrometers while its thickness and the gap between the ring and driving/sensing electrodes are only about several micrometers. (Tao, 2011, Esmaeili, 2006, and Ayazi, 2000) Therefore, it is reasonable to adopt the thin ring theory and assume the electric field between the ring and electrode to be uniform. Since the operation of a vibratory ring gyroscope relies on its first two bending-dominant vibrational modes, then it is reasonable to assume the ring to be inextensible. The proposed analytical model is based on thin-ring theory and derived by means of Hamilton’s principle.

Before the vibration analysis, the authors study the static equilibrium of a stationary ring under electric

Paper Received September, 2020. Revised October, 2020. Accepted October, 2020. Author for Correspondence: Yuh-Chung Hu.

* *Associate professor, School of Mechatronics and Automobile Engineering, Yantai University, Yantai 264005, China*

** *Graduate student, School of Mechatronics and Automobile Engineering, Yantai University, Yantai 264005, China*

*** *Professor, Department of Mechanical and Electro-Mechanical Engineering, National ILan University, ILan, 26047 Taiwan*

field to find the static pull-in voltage of the stationary ring. A linearized model of electric field is also derived and agrees very well with the non-linear electric field model at the voltage being lower than the static pull-in voltage. Therefore, the linearized electric field model is adopted to the vibration analysis of the rotating ring under uniform electric field before pull-in. The dynamic instabilities of the rotating ring before static pull-in are studied as well. By considering the initial stress induced by centrifugal force, one can find that the dynamics of the rotating ring is very different from the model ignoring the initial stress, such as the natural frequencies and traveling speeds of the vibrational modes and the dynamic stabilities before static pull-in and the difference is significant at high rotational speed. Thus, the initial stress induced by centrifugal force cannot be ignored at high rotational speed. The most interesting is that once the voltage between the rotating ring and electrode enters the unstable region, one can further raise the rotational speed to higher than the critical speed to escape the unstable region. This situation didn't appear in the model ignoring the initial stress.

STATIC PULL-IN PHENOMENON

This section details the static pull-in phenomenon of a stationary ring under a uniform electric field. This is an electromechanical coupling problem because the deflection of the ring affects the electric field and the vice versa. In this section, the static pull-in voltage due to the non-linear electric field is derived firstly. Then a linearized model of the electric field is derived based on the assumption of small deformation. A comparison of the non-linear and linearized models of the electric field is made, which depict that the linearized model agrees well with the non-linear model before static pull-in.

Assumptions

Consider the stationary ring shown in Fig. 1(a). The ring's radius, a, is much larger than its thickness, h, and the gap, g, between the ring and fixed electrode is of the same order of magnitude of the ring's thickness. A uniform electric field along the radial direction is produced by exerting an electrical potential difference between the ring and electrode (hereinafter simply referred to as "voltage"). This subsection deals with the static equilibrium problem of the stationary ring. According to thin-ring theory, the plane sections of the ring remain plane after deformation and normal to the neutral surface, the shear deformation in transverse direction is negligible and the only significant strain is in the circumferential direction. The inertia of the stationary ring is neglected for static equilibrium problem. X-Y is a stationary coordinate system; u_θ and u_3 denote the circumferential and transverse deflections of the ring respectively; ψ is the angular position on the ring with respect to the stationary coordinate system; b denotes the width of the ring respectively.

Non-linear Model

For a stationary ring subjected to uniform electric field in static equilibrium, the mechanical strain energy per unit width is (Huang, 1987)

$$U=\int_0^{2\pi}\left[\frac{K}{2a^2}(u_\theta'+u_3)^2+\frac{D}{2a^4}(u_\theta'-u_3'')^2\right]ad\theta\ ,\qquad(1)$$

wherein $D = Eh^3/12$ is bending stiffness and $K = Eh$ is membrane stiffness. The electric potential energy stored in the electric field is (Hu, 2004, 2006)

$$U_e=-\int_0^{2\pi}\frac{1}{2}\frac{\varepsilon V^2}{g-u_3}ad\theta\ .\qquad(2)$$

Therefore, the total energy, L, of the system is given by

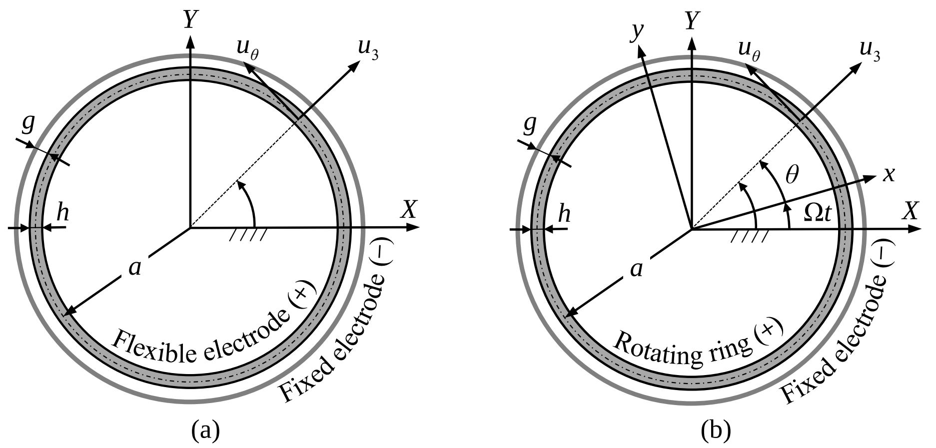

Fig. 1. The schematic diagram of a ring surrounded by a circular fixed electrode; (a) a stationary (non-rotating) ring; (b) a rotating ring with the rotational speed Ω.

$$
\begin{aligned}
L &= U + U_e \\
&= \int_0^{2\pi}\left[\frac{K}{2a^2}(u'_\theta + u_3)^2 + \frac{D}{2a^4}(u'_\theta - u''_3)^2\right] a\,d\theta \quad (3) \\
&\quad -\int_0^{2\pi}\frac{1}{2}\frac{\varepsilon V^2}{g-u_3} a\,d\theta.
\end{aligned}
$$

Since the electric field distributes uniformly around the ring and along its radial direction, then the ring's static deformation under the uniform electric field is uniform and symmetrical with respect to the center of the ring. Thus, the static deflection of the ring is much like the so-called breathing mode of a ring (Soedel, 2005) and one can assume the ring's deflection shape as the breathing mode, namely both u_3 and u_θ are constants. By the assumed mode method, the total energy of the ring can be written as:

$$
\begin{aligned}
L &= \int_0^{2\pi}\frac{K\delta^2}{2a^2} a\,d\theta - \int_0^{2\pi}\frac{1}{2}\frac{\varepsilon V^2}{g-\delta} a\,d\theta \\
&= \frac{\pi K\delta^2}{a} - \frac{\pi\varepsilon a V^2}{g-\delta},
\end{aligned} \quad (4)
$$

where δ, a constant, is the deflection of the stationary ring. The total energy is a function of the ring's deflection. Both the first- and second-order derivatives of the total energy with respect to δ have to be zero at the transition from stable to unstable equilibrium (Hu, 2006), i.e.

$$
\begin{cases}
\dfrac{dL}{d\delta} = 0 \Rightarrow 2\bar{\delta}(1-\bar{\delta})^2 = \bar{V}_0^{\,2}, \\
\dfrac{d^2L}{d\delta^2} = 0 \Rightarrow (1-\bar{\delta})^3 = \bar{V}_0^{\,2},
\end{cases} \quad (5)
$$

wherein $\bar{\delta}$ and $\bar{V}_0$ are respectively the dimensionless deflection and the dimensionless voltage,

$$
\bar{\delta} = \delta/g,\ \bar{V}_0 = \frac{\sqrt{\varepsilon V^2/(\rho h g^3)}}{\omega_{f0}},\ \omega_{f0} = \sqrt{\frac{K}{\rho h a^2}}, \quad (6)
$$

and ω_{f0} is the natural frequency of the breathing mode. The static pull-in is an unstable equilibrium state of a micro structure subjected to electrostatic force. By solving equation (5), one can obtains the dimensionless static pull-in voltage, $\bar{V}_{in}$, and the corresponding dimensionless static pull-in deflection, $\bar{\delta}_{in}$:

$$
\bar{V}_{in} = \sqrt{\frac{8}{27}} \approx 0.54,\quad \bar{\delta}_{in} = \frac{1}{3}. \quad (7)
$$

Linearized Model

By means of Taylor's series expansion, one can expand the term, $1/(g-u_3)$, in the electric potential energy with respect to the initial position, namely $u_3 = 0$:

$$
\frac{1}{g-u_3} = \frac{1}{g} + \frac{u_3}{g^2} + \frac{u_3^2}{g^3} + \frac{u_3^3}{g^4} + \cdots, \quad (8)
$$

and truncates the third- and higher-order terms. Then, the electric potential energy is linearized to be

$$
U_e = -\int_0^{2\pi}\frac{1}{2}\varepsilon V^2\left(\frac{1}{g} + \frac{u_3}{g^2} + \frac{u_3^2}{g^3}\right) a\,d\theta, \quad (9)
$$

and the total energy becomes

$$
\begin{aligned}
L &= U + U_e \\
&= \int_0^{2\pi}\left[\frac{K}{2a^2}(u'_\theta + u_3)^2 + \frac{D}{2a^4}(u'_\theta - u''_3)^2\right] a\,d\theta \quad (10) \\
&\quad -\int_0^{2\pi}\frac{1}{2}\varepsilon V^2\left(\frac{1}{g} + \frac{u_3}{g^2} + \frac{u_3^2}{g^3}\right) a\,d\theta.
\end{aligned}
$$

Similar to the previous subsection, by the assumed mode method, the total energy of the ring can be written as:

$$
\begin{aligned}
L &= \int_0^{2\pi}\frac{K\delta^2}{2a^2} a\,d\theta - \int_0^{2\pi}\frac{1}{2}\varepsilon V^2\left(\frac{1}{g} + \frac{\delta}{g^2} + \frac{\delta^2}{g^3}\right) a\,d\theta \\
&= \frac{\pi K\delta^2}{a} - \pi\varepsilon a V^2\left(\frac{1}{g} + \frac{\delta}{g^2} + \frac{\delta^2}{g^3}\right).
\end{aligned} \quad (11)
$$

The first-order derivative of the total energy with respect to δ has to be zero in static equilibrium (Hu, 2006), i.e.

$$
\frac{dL}{d\delta} = 0 \Rightarrow \frac{2\bar{\delta}}{(1+2\bar{\delta})} = \bar{V}_0^{\,2} \Rightarrow \bar{\delta} = \frac{\bar{V}_0^{\,2}}{2(1-\bar{V}_0^{\,2})}, \quad (12)
$$

where the dimensionless voltage, $\bar{V}_0$, and deflection, $\bar{\delta}$, are defined as equation (6).

Comparison of the Non-linear and Linearized Models of Electric Field

A comparison of the non-linear and linearized electric field model is made. Although equation (7) gives a closed-form solution for the voltage and deflection at static pull-in, one has to solve the first part of equation (5) to get the deflection at a certain value of the voltage before pull-in. It is inconvenient to solve the first part of equation (5) because of the cubic equation. The cubic equation has three roots and which one is correct still require determining based on physical insight. Equation (12) gives an explicit and easy-to-use solution for the stable equilibrium before pull-in though the nonlinear static pull-in phenomenon of electric field disappears. Fig. 2(a) shows the comparison of the deflections obtained by the two

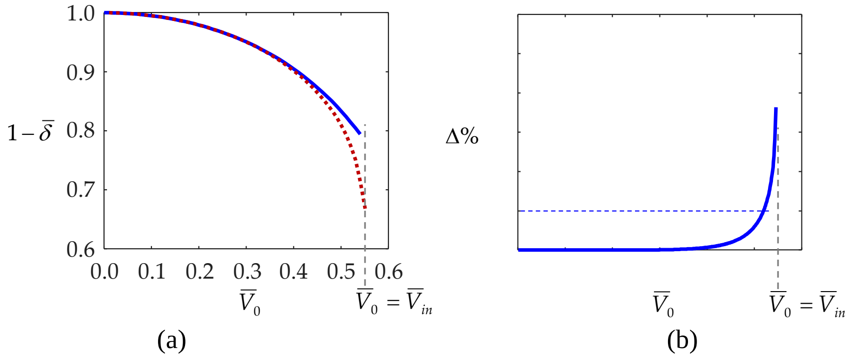

Fig. 2. Comparison of the static equilibrium given by non-linear (dashed curve) and linearized (solid curve) models of the electric field; (a) the deflections of the stationary ring versus the voltage; (b) the percentage deviation of the linearized model from the non-linear model. Both the abscissa and ordinate are dimensionless.

electric field models, wherein the dashed curve is obtained by the non-linear model, equation (5), and the solid curve is obtained by the linearized model, equation (12). The non-linear model has the pull-in phenomenon occurring at $\bar{V}_{in} = \sqrt{8/27}$ while the linearized one doesn't. Fig. 2(b) shows that the percentage deviation of the linearized model from the non-linear one is small, less than 5%, before pull-in. Thus, the linearized model of electric field is an acceptable approximation before static pull-in. The linearized electric field model for the case of micro cantilever beam had been validated by experiment in Hu's published paper (Hu, 2004). In the following text, the authors will adopt the linearized electric field model to investigate the vibration of a rotating ring subjected to uniform electric field at the voltage that is lower than the static pull-in voltage.

DYNAMIC MODELS

This section details the derivation of equation of motion for a rotating ring subjected to uniform electric field. What the authors concerned is the rotating ring's vibration. The linearized model of electric field given by the subsection of Linearized Model is adopted. Based on thin-ring theory and inextensible approximation, the analytical model of the rotating ring subjected to a uniform electric field in radial direction is derived by means of Hamilton's principle. This is an electromechanical coupling problem because the deflection of the ring will affect the electric field and the vice versa. Consider a ring rotating at the speed of Ω, shown in Fig. 1(b). The basic assumptions are similar to that of the section of STATIC PULL-IN PHENOMENON except that the translational inertia of the rotating ring is considered. A rotational coordinate system x-y rotating with the ring is added and θ denotes the angular position on the ring with respect to the rotational coordinate system.

Energy Expressions

The kinetic energy, T, and strain energy, U, per unit width of the rotating ring are given by (Huang, 1987)

$$T = \frac{1}{2}\rho ha\int_0^{2\pi}\left[\left(\dot{u}_3 - u_\theta\Omega\right)^2 + \left(\dot{u}_\theta + u_3\Omega + a\Omega\right)^2\right]d\theta, \tag{13}$$

$$\begin{aligned} U &= \int_0^{2\pi}\left[\frac{K}{2a^2}(u_\theta' + u_3)^2 + \frac{D}{2a^4}(u_\theta' - u_3'')^2\right]ad\theta \\ &+\int_0^{2\pi}\rho a^2\Omega^2 h\frac{1}{a}(u_\theta' + u_3)ad\theta \\ &+\int_0^{2\pi}\rho a^2\Omega^2 h\frac{1}{2a^2}\left[(u_\theta' + u_3)^2 + (u_3' - u_\theta)^2\right]ad\theta, \end{aligned} \tag{14}$$

wherein the second integral of the strain energy is due to the initial stress, $\rho a^2\Omega^2$, induced by rotational centrifugal force. The initial stress induced by centrifugal force is hereinafter simply referred to as "initial stress." By the use of the linearized electric field model derived in the subsection of Linearized Model, the work done of the electric field on the rotating ring per unit width is

$$W = \int_0^{2\pi}\frac{\varepsilon V^2}{2}\left(\frac{1}{g} + \frac{u_3}{g^2} + \frac{u_3^2}{g^3}\right)ad\theta, \tag{15}$$

wherein ε is the permittivity of free space. This work is exactly the negative of the electric potential energy stored in the electric field because the electric field is a conservative field.

Dynamic Equations of Motion

If the motion of the rotating ring was along a varied path deviating slightly from the true path, then the variations of the aforesaid energy expressions were

$$\begin{aligned} \delta T = \rho ha\int_0^{2\pi}\Big[&\left(\dot{u}_\theta + u_3\Omega + a\Omega\right)\Omega\delta u_3 + \left(\dot{u}_3 - u_\theta\Omega\right)\delta\dot{u}_3 \\ &-\left(\dot{u}_3 - u_\theta\Omega\right)\Omega\delta u_\theta + \left(\dot{u}_\theta + u_3\Omega + a\Omega\right)\delta\dot{u}_\theta\Big]d\theta, \end{aligned} \tag{16}$$

$$\delta U = \int_0^{2\pi}\left[\frac{K}{a^2}(u_\theta' + u_3) + \rho a\Omega^2 h + \rho\Omega^2 h(u_\theta' + u_3)\right.$$
$$\left. - \rho\Omega^2 h(u_3'' - u_\theta') - \frac{D}{a^4}(u_\theta''' - u_3'''')\right]\delta u_3 a d\theta \tag{17}$$
$$-\int_0^{2\pi}\left[\frac{K}{a^2}(u_\theta'' + u_3') + \frac{D}{a^4}(u_\theta'' - u_3''')\right.$$
$$\left. + \rho\Omega^2 h(u_\theta'' + u_3') + \rho\Omega^2 h(u_3' - u_\theta)\right]\delta u_\theta a d\theta,$$

$$\delta W = \int_0^{2\pi}\frac{\varepsilon V^2}{2}\left(\frac{1}{g^2} + \frac{2u_3}{g^3}\right)\delta u_3 a d\theta\,. \tag{18}$$

The so-called varied path is a small deviation in deflection with respect to the true path in the same time duration. Hamilton's principle (Meirovitch, 1967) says that the true path of a continuous system between the two specified states at two time instants causes the integral of the variation of total energy in time is invariant along all possible varied paths, that is

$$\int_{t_0}^{t_1}(\delta U - \delta T - \delta W)dt = 0\,. \tag{19}$$

which gives rise to

$$\int_{t_0}^{t_1}\int_0^{2\pi}\left\{-\frac{D}{a^4}(u_\theta''' - u_3'''') + \frac{K}{a^2}(u_\theta' + u_3)\right.$$
$$+ \rho h(\ddot{u}_3 - 2\dot{u}_\theta\Omega - u_3\Omega^2 - a\Omega^2)$$
$$- \frac{\varepsilon V^2}{2}\left(\frac{1}{g^2} + \frac{2u_3}{g^3}\right)$$
$$\left. + \rho a\Omega^2 h + \rho\Omega^2 h(u_3 + 2u_\theta' - u_3'')\right\}\delta u_3 a d\theta dt \tag{20}$$
$$+\int_{t_0}^{t_1}\int_0^{2\pi}\left\{-\frac{D}{a^4}(u_\theta'' - u_3''') - \frac{K}{a^2}(u_\theta'' + u_3')\right.$$
$$+ \rho h(\ddot{u}_\theta + 2\dot{u}_3\Omega - u_\theta\Omega^2)$$
$$\left. + \rho\Omega^2 h(u_\theta - 2u_3' - u_\theta'')\right\}\delta u_3 a d\theta dt = 0.$$

This equation was satisfied only if each of the integrand in the double integrals equals zero and thus gives rise to the equations of motion:

$$\frac{D}{a^4}(u_3'''' - u_\theta''') + \frac{K}{a^2}(u_\theta' + u_3) + \rho h(\ddot{u}_3 - 2\Omega\dot{u}_\theta)$$
$$+ \rho h\Omega^2(2u_\theta' - u_3'') - \frac{\varepsilon V^2}{g^3}u_3 = \frac{\varepsilon V^2}{2g^2}, \tag{21}$$

$$\frac{D}{a^4}(u_3''' - u_\theta'') - \frac{K}{a^2}(u_\theta'' + u_3')$$
$$+ \rho h(\ddot{u}_\theta + 2\Omega\dot{u}_3) + \rho h\Omega^2(-2u_3' - u_\theta'') = 0. \tag{22}$$

The terms with Ω are induced by the effects of rotational motion, including the Coriolis force and centrifugal force, and the terms with V are induced by the electric field. Equations (21) and (22) could be reduced to the case of a rotating ring without electric field derived by Huang (Huang, 1987) if set $V = 0$. That case had been validated with experimental data in Huang's paper. The most interesting of the present model is that the electric field causes an equivalent negative stiffness, $-\varepsilon V^2/g^3$, which will soften the ring.

Since the uniform electrical field is along the radial direction of the ring, then there is no circumferential forcing on the ring. So the transverse vibration (bending modes) is predominant in the present case. Substitute equation (21) into equation (22) and use the inextensible approximation (Soedel, 2005),

$$u_\theta' = -u_3\,, \tag{23}$$

to eliminate u_θ. One can obtain an equation of motion of a rotating ring under uniform electric field based on inextensible approximation:

$$\frac{D}{a^4}\left(\frac{\partial^6 u_3}{\partial\theta^6} + 2\frac{\partial^4 u_3}{\partial\theta^4} + \frac{\partial^2 u_3}{\partial\theta^2}\right) - \frac{\varepsilon V^2}{g^3}\frac{\partial^2 u_3}{\partial\theta^2}$$
$$+ \rho h\left[\left(\frac{\partial^4 u_3}{\partial\theta^2\partial t^2} + 4\Omega\frac{\partial^2 u_3}{\partial\theta\partial t} - \frac{\partial^2 u_3}{\partial t^2}\right) - \Omega^2\left(3\frac{\partial^2 u_3}{\partial\theta^2} + \frac{\partial^4 u_3}{\partial\theta^4}\right)\right] = 0. \tag{24}$$

NATURAL FREQUENCIES AND DYNAMIC STABILITIES

This section details the derivation of the natural frequencies for a rotating ring under a uniform electric field. As mentioned in the section of DYNAMIC MODELS, the electric field will introduce an equivalent negative stiffness to the rotating ring and thus soften it. For a non-rotating ring, only one natural frequency corresponds to each wave number n. However, the rotation effect will make the natural frequency to each wave number n splitting into two frequencies, one corresponds to the forward traveling mode and another one to the backward traveling mode. The traveling modes will be discussed in the following section. The section of STATIC PULL-IN PHENOMENON reveals that a stationary ring will be pulled in when the voltage larger than the so-called static pull-in voltage, which is a statically unstable equilibrium between the mechanical restoring force and electrostatic force. Hereinafter, the authors will discuss only the vibration of the rotating ring at a voltage lower than the static pull-in voltage. This section will discuss the vibration of a rotating ring subjected to a uniform electric field. The rotating ring will reach dynamically unstable equilibrium at certain values of rotational speeds and voltages even though the voltage lower than the static pull-in voltage, $\bar{V}_{in}$. Besides, the effects of initial stress on the natural frequencies and dynamic stabilities of the rotating ring will also be discussed.

Due to the geometrical periodicity, one can assume the deflection function of the rotating ring to be

$$u_3(\theta,t)=A_n e^{j(n\theta+\omega_n t)}. \tag{25}$$

Substituting it into equation (24) yields the frequency equation,

$$\begin{aligned}&\omega_n^2-\frac{4n\Omega}{(n^2+1)}\omega_n-\frac{n^2\left(n^2-1\right)^2}{(n^2+1)}\frac{D}{\rho h a^4}\\&+\frac{n^2}{(n^2+1)}\frac{\varepsilon V^2}{\rho h g^3}+\frac{n^2(3-n^2)\Omega^2}{(n^2+1)}=0.\end{aligned} \tag{26}$$

There are two natural frequencies, ω_{n1} and ω_{n2}, for each wave number n,

$$\begin{aligned}\omega_{n1}=&\frac{2n\Omega}{(n^2+1)}\\&-\sqrt{\frac{n^2\left(n^2-1\right)^2}{(n^2+1)}\frac{D}{\rho h a^4}-\frac{n^2}{(n^2+1)}\frac{\varepsilon V^2}{\rho h g^3}+\frac{n^2(n^2-1)^2}{(n^2+1)^2}\Omega^2},\end{aligned} \tag{27}$$

$$\begin{aligned}\omega_{n2}=&\frac{2n\Omega}{(n^2+1)}\\&+\sqrt{\frac{n^2\left(n^2-1\right)^2}{(n^2+1)}\frac{D}{\rho h a^4}-\frac{n^2}{(n^2+1)}\frac{\varepsilon V^2}{\rho h g^3}+\frac{n^2(n^2-1)^2}{(n^2+1)^2}\Omega^2}.\end{aligned} \tag{28}$$

It is obvious that only one natural frequency for each wave number, n, if $\Omega=0$. Therefore, the rotation effect will make the natural frequency for each wave number splitting into two different frequencies. This is due to the Coriolis acceleration. For the flexural modes ($n\geq 2$), equations (27) and (28) can be expressed as

$$\frac{\omega_{nk}}{\omega_{fn}}=\frac{2n}{(n^2+1)}\bar{\Omega}_n\mp\sqrt{1-\frac{n^2}{(n^2+1)}\bar{V}_n^2+\frac{n^2(n^2-1)^2}{(n^2+1)^2}\bar{\Omega}_n^2} \tag{29}$$

for k = 1, 2, wherein $\bar{\Omega}_n$ is the dimensionless rotational speed, $\bar{V}_n$ is the dimensionless voltage, and ω_{fn} is the natural frequencies of the case of Ω = 0 and V = 0,

$$\bar{\Omega}_n=\frac{\Omega}{\omega_{fn}},\ \bar{V}_n=\frac{\sqrt{\varepsilon V^2/(\rho h g^3)}}{\omega_{fn}},\ \omega_{fn}=\sqrt{\frac{n^2\left(n^2-1\right)^2}{(n^2+1)}\frac{D}{\rho h a^4}}. \tag{30}$$

To avoid confusion, it should be mentioned here that the dimensionless voltage, $\bar{V}_n$, is different from the one, $\bar{V}_0$, defined by equation (6) for the case of static equilibrium mentioned in Section 2. $\bar{V}_n$ depends on the waver number n, while $\bar{V}_0$ doesn't. Their relationship is:

$$\frac{\bar{V}_n}{\bar{V}_0}=\frac{a}{h}\sqrt{\frac{12(n^2+1)}{n^2\left(n^2-1\right)^2}}. \tag{31}$$

To ensure the two natural frequencies given by equation (29) for each wave number n are real numbers, $\bar{\Omega}_n$ and $\bar{V}_n$ have to satisfy the following equation:

$$\frac{\bar{V}_n^{\,2}}{(n^2+1)/n^2}-\frac{\bar{\Omega}_n^{\,2}}{(1/n^2)(n^2+1)^2/(n^2-1)^2}\leq 1, \tag{32}$$

otherwise, the natural frequencies are a pair of complex conjugate, namely the form of $\alpha-j\beta$ and $\alpha+j\beta$, wherein the latter renders the vibration amplitude decaying with time and the former makes it diverging with time, namely unstable. Fig. 3(a) shows the schematic diagram of equation (32). Between the stable and unstable regions is a quarter hyperbola curve named as the "critical curve" by the authors. The stability of the rotating ring is determined by $\bar{\Omega}_n$ and $\bar{V}_n$; it was critical stable if $\bar{\Omega}_n$ and $\bar{V}_n$ fell on the critical curve; stable if fell in the upper-left side of the critical curve; and unstable if fell in the lower-right side of the critical curve. In the stable region, there are two distinct real-number natural frequencies for each wave number n, while on the critical curve are two identical real-number natural frequencies for each wave number. The critical curve will approach to the

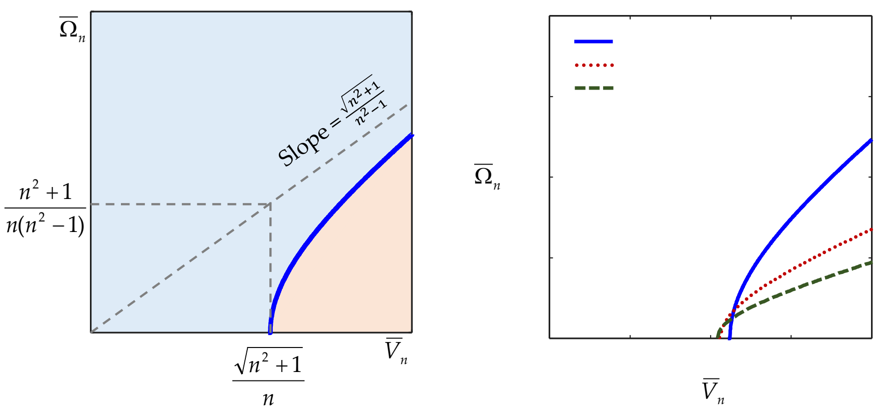

Fig. 3. (a) The schematic diagram of the dynamic stability of the rotating ring subjected to uniform electric field. (b) The critical curves for the first three flexural modes.

asymptote with the slope of $\sqrt{n^2+1}/(n^2-1)$. The vibration of the rotating ring is stable when $\bar{V}_n \le \sqrt{n^2+1}/n$. The most interesting is that once the value of the dimensionless voltage enters the unstable region, namely $\bar{V}_n > \sqrt{n^2+1}/n$, one can further raises the rotational speed higher than the critical curve to escape the unstable region. As mentioned in the section of DYNAMIC MODELS, the electric field introduces an equivalent negative stiffness, $-\varepsilon V^2/g^3$, into the rotating ring and thereby make it softer and more unstable. However, the initial stress, $\rho a^2\Omega^2$, induced by centrifugal force is proportional to the square of the rotational speed and thereby make the rotating ring more rigid. This is why raising the rotational speed will change the vibration of the rotating ring from unstable to stable. Fig. 3(b) shows the critical curves of the first three flexural modes.

To get intuitive feeling of the effect of electric field on the natural frequencies, let $\bar{\Omega}_n = 0$ in equation (29), namely the case of non-rotating ring. Fig. 4(a) shows that the absolute values of the dimensionless frequency, $|\omega_{nk}/\omega_{fn}|$, are functions of the dimensionless voltage, $\bar{V}_n$, and which are concave-down parabola. Therefore, the electric field decreases the natural frequency due to its equivalent negative stiffness. Now, look at Fig. 4(b), the schematic diagram of the absolute values of the dimensionless frequency, $|\omega_{nk}/\omega_{fn}|$, given by equation (29). Two natural frequencies exit for each wave number, n, if $\bar{\Omega}_n \ne 0$. The lower frequency corresponds to the forward traveling mode and the higher one to the backward traveling mode. The introduction of electric field, $\bar{V}_n \ne 0$, will simultaneously reduce the natural frequencies of the forward and backward traveling modes due to its equivalent negative stiffness. The traveling modes will be discussed in the following section. Fig. 5 shows the natural frequencies of the first three flexural modes for the rotating ring under uniform electric field.

NATURAL MODES

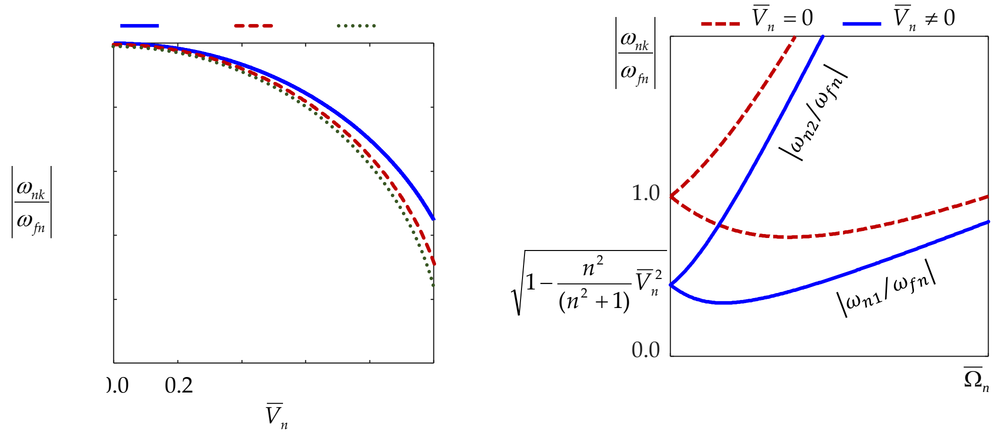

(a) (b)

Fig. 4. The effects of electric field and rotational speed on the natural frequency of a rotating ring subjected to uniform electric field; (a) the natural frequencies of a non-rotating ring (Ω = 0) subjected to uniform electric field; (b) the schematic diagram of the natural frequencies of a rotating ring subjected to uniform electrical field.

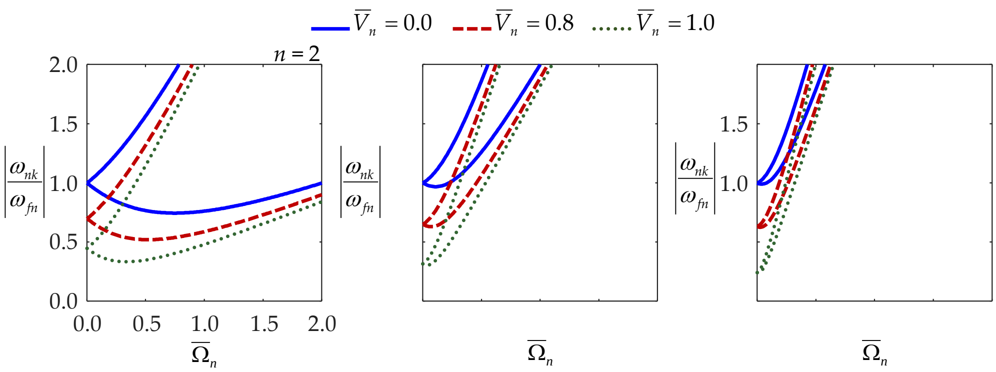

(a) (b) (c)

Fig. 5. The natural frequencies, given by equation (29), of a rotating ring subjected to uniform electric field. (a) the first flexural mode, n = 2; (b) the second flexural mode, n = 3; (c) the third flexural mode, n = 4.

This section details the derivation of the natural modes of the rotating ring under a uniform electric field. The natural modes are usually not functions of time. However, the modes defined in the following text are functions of time. Such time-dependent modes were named as the traveling modes by Huang (Huang, 1987). The traveling modes travel either in the same or opposite directions of the rotating ring when observe at an absolute coordinate system.

Natural Modes

To observe the natural modes at the absolute coordinate system, transform equation (25) into the absolute coordinate system by the relation of $\psi = \theta + \Omega t$:

$$u_{3k}(\psi, t) = A_{nk} e^{jn[\psi - (\Omega - \omega_{nk}/n)t]}, \tag{33}$$

for k = 1, 2. The modes defined in equation (33) are functions of time. Such time-dependent modes were named as traveling modes by Huang (Huang, 1987). The traveling modes travel either in the same or opposite directions of the rotating ring to an observer at absolute coordinate system. To explain the velocities of the traveling modes, the authors set $A_{nk} = 1$ and take the real part of equation (33),

$$\cos n[\psi - (\Omega - \omega_{nk}/n)t]. \tag{34}$$

Set to its maximum value, 1, to see at what velocity the antinodes of modes travel:

$$\cos n[\psi - (\Omega - \omega_{nk}/n)t] = 1. \tag{35}$$

This gives

$$\psi_{\max} = 2m\pi/n + (\Omega - \omega_{nk}/n)t, \tag{36}$$

where m = 0, 1, 2, 3, … etc. Therefore, with respect to the absolute coordinate system, the modes travel at the velocities of

$$\begin{aligned}\dot{\psi}_{\max 1} &= \Omega - \frac{\omega_{n1}}{n} = \frac{(n^2-1)}{(n^2+1)}\Omega \\ &+ \frac{1}{n}\sqrt{\frac{n^2(n^2-1)^2}{(n^2+1)}\frac{D}{\rho h a^4} - \frac{n^2}{(n^2+1)}\frac{\varepsilon V^2}{\rho h g^3} + \frac{n^2(n^2-1)^2}{(n^2+1)^2}\Omega^2},\end{aligned} \tag{37}$$

$$\begin{aligned}\dot{\psi}_{\max 2} &= \Omega - \frac{\omega_{n2}}{n} = \frac{(n^2-1)}{(n^2+1)}\Omega \\ &- \frac{1}{n}\sqrt{\frac{n^2(n^2-1)^2}{(n^2+1)}\frac{D}{\rho h a^4} - \frac{n^2}{(n^2+1)}\frac{\varepsilon V^2}{\rho h g^3} + \frac{n^2(n^2-1)^2}{(n^2+1)^2}\Omega^2}.\end{aligned} \tag{38}$$

For the flexural modes ($n \geq 2$), equations (37) and (38) can be expressed as (for k = 1, 2)

$$\begin{aligned}\frac{\dot{\psi}_{\max k}}{\omega_{fn}} &= \frac{(n^2-1)}{(n^2+1)}\bar{\Omega}_n \\ &\pm \frac{1}{n}\sqrt{1 - \frac{n^2}{(n^2+1)}\bar{V}_n^2 + \frac{n^2(n^2-1)^2}{(n^2+1)^2}\bar{\Omega}_n^2}.\end{aligned} \tag{39}$$

There are three possibilities of the velocities of traveling modes, i.e. stationary ($\dot{\psi}_{\max} = 0$), traveling in the same direction but lag behind the rotating ring ($\dot{\psi}_{\max} > 0$), and traveling in the direction opposite to the rotating ring ($\dot{\psi}_{\max} < 0$). Table 1 summarizes the three possibilities and the corresponding criteria. The modes became stationary if the voltage satisfied equation (40). This means that the modes do not rotate but appear as a stationary deflection of the ring to an observer at the absolute coordinate system. The corresponding stationary modes are simply cosine functions, cos($n\psi$). Fig. 6 illustrates the first three stationary flexural modes of the rotating ring. If the voltage satisfied equation (41), then the traveling velocities of modes were positive and the modes travel in the same direction of the rotating ring. If the voltage satisfied equation (42), then the traveling velocities of modes were negative and the modes travel in the direction opposite to the rotating ring. The following text will deal with the case of the voltage lies in the dynamic stable region, namely $\bar{V}_n < \sqrt{n^2+1}/n$, so that the cases satisfying equations (40) and (41) will not occur.

For $\Omega - \omega_{nk}/n \neq 0$, there are two traveling

Table 1. The characteristics and physical meanings of the velocities of traveling modes.

Signs of the traveling speeds of modes	**Physical meanings**	**Criteria**
$\dot{\psi}_{\max} = \Omega - \omega_{nk}/n = 0$	Stationary modes.	$\bar{V}_n = \sqrt{n^2+1}/n$ (1)
$\dot{\psi}_{\max} = \Omega - \omega_{nk}/n > 0$	The modes travel in the same direction of the rotating ring but lag behind it.	$\bar{V}_n > \sqrt{n^2+1}/n$ (2)
$\dot{\psi}_{\max} = \Omega - \omega_{nk}/n < 0$	The modes travel in the direction opposite to the rotating ring.	$\bar{V}_n < \sqrt{n^2+1}/n$ (3)

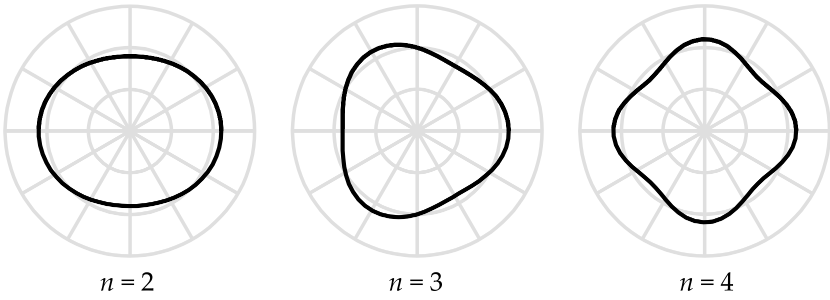

(a) (b) (c)

Fig. 6. The stationary modes given by the mode shape function, $\cos(n\psi)$, when $\bar{V}_n$ satisfy equation (40).

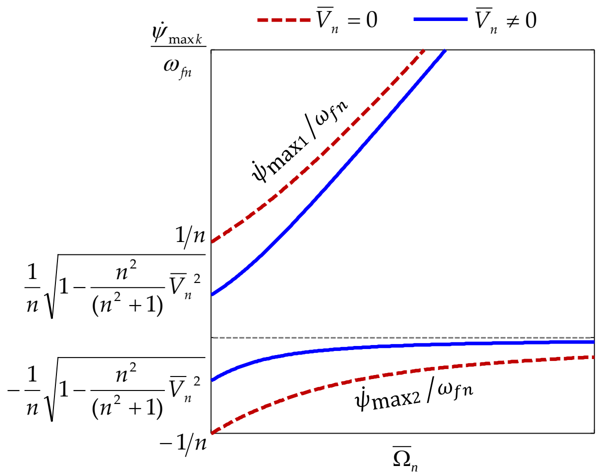

Fig. 7. The schematic diagram of the traveling velocities of modes, given by equation (39), of the forward (upper branches) and backward (lower branches) traveling modes.

modes for each wave number n:

$$\cos n(\psi - \dot{\psi}_{\max 1} t), \quad \cos n(\psi - \dot{\psi}_{\max 2} t), \quad (43)$$

where the velocities of the two traveling modes are given by equation (39). Fig. 7 shows the schematic diagram of the dimensionless traveling velocity of modes, $\dot{\psi}_{\max k}/\omega_{fn}$, when the voltage lies in the stable region ($\bar{V}_n < \sqrt{n^2+1}/n$). The dashed curves illustrate the case of $\bar{V}_n = 0$ while the solid curves illustrate the case of $\bar{V}_n \neq 0$. The upper branches are forward traveling modes while the lower ones are backward traveling modes. Both the electric field and ring's rotational speeds affect the velocities of the traveling modes. The electric field simultaneously reduces the speeds of the forward and backward traveling modes. The rotation effect makes the speeds of the forward and backward traveling modes different. The rotational speed of the ring raises the speed of the forward traveling mode while lower that of the backward traveling mode. Fig. 8 shows the traveling

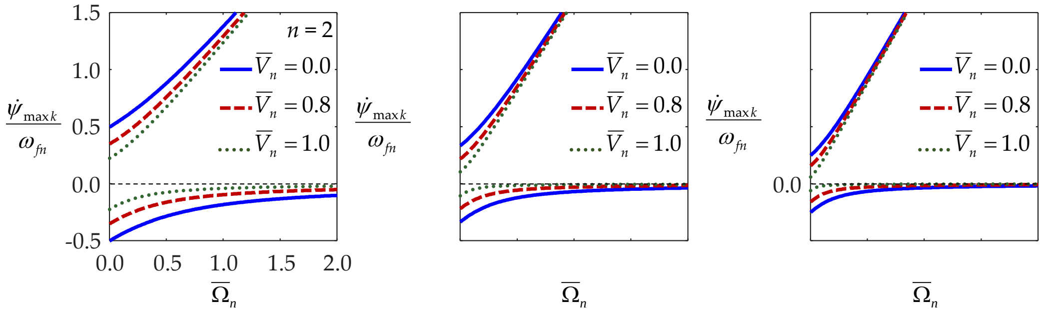

(a) (b) (c)

Fig. 8. The traveling velocities of modes, given by equation (39), of the forward (upper branches) and backward (lower branches) traveling modes in the stable region, $\bar{V}_n < \sqrt{n^2+1}/n$; (a) the first flexural mode, n = 2; (b). the second flexural mode, n = 3; (c) the third flexural mode, n = 4.

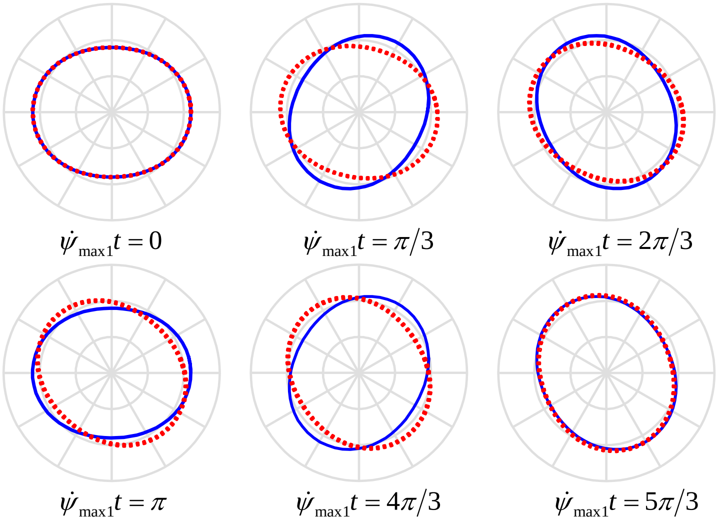

Fig. 9. The traveling modes of n = 2 at various instance of time viewed at an absolute coordinate system, the blue curve is the forward traveling mode, traveling in counterclockwise, while the red one is the backward traveling mode, traveling in clockwise.

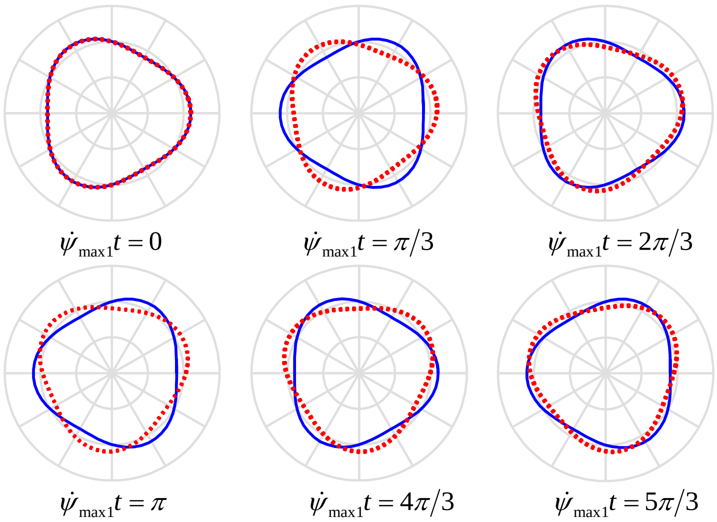

Fig. 10. The traveling modes of n = 3 at various instance of time viewed at an absolute coordinate system, the blue curve is the forward traveling mode, traveling in counterclockwise, while the red one is the backward traveling mode, traveling in clockwise.

speeds of the first three flexural modes in the stable region, $\bar{V}_n < \sqrt{n^2+1}/n$. Figures 9 and 10 show the traveling modes of the wave numbers n = 2 and 3 respectively, the forward and backward traveling modes travel in opposite directions. The forward traveling modes travel in counterclockwise while the backward ones in clockwise.

CONCLUSIONS

This paper derives an analytical model, which considers the initial stress induced by the rotational centrifugal force, for a rotating ring subjected to the uniform electric field along the radial direction. The static and dynamic stabilities of stationary and rotating rings subjected to uniform electric field are investigated. In addition to the effects of rotation and electric field, the effect of initial stress induced by rotational centrifugal force on the vibration of a rotating ring are discussed. The present analytical model can be reduced to a simply rotating ring model by setting the voltage to be zero. It can also be further reduced to a simply non-rotating ring model by setting both the voltage and rotational speed to zero. Based on the results of the present analytical model, some conclusions are proposed in the following.

For the static equilibrium problem of a stationary ring under uniform electric field, the authors derive a non-linear and a linearized model of the electric field. According to the non-linear electric field model, the dimensionless pull-in voltage of the stationary ring is $\sqrt{8/27}$ and the corresponding dimensionless pull-in deflection is 1/3. The linearized electric field model agrees very well with the non-linear one before pull-in, whose relative deviation less than 5% before pull-in. Therefore, the linearized electric field model is adopted in the vibration analysis of a rotating ring subjected to uniform electric field at the voltage that is lower than the static pull-in voltage.

For the vibration of a rotating ring subjected to uniform electric field, the electric field causes an equivalent negative stiffness that is proportional to the square of the voltage. The equivalent negative stiffness will soften the rotating ring and thereby probably make the rotating ring unstable. The rotation effect makes the natural frequencies of the forward and backward traveling modes for each wave number different. Furthermore, the rotation will induce an initial stress due to the centrifugal force, which is proportional to the square of the rotational speed. Therefore, the stability of a rotating ring subjected to uniform electric field is determined by rotational speed and voltage. Once the voltage enters the unstable region, one can further raise the rotational speed higher than the critical speed to escape the stable region. This is due to that the initial stress induced by centrifugal force is proportional to the square of the rotational speed. According to the comparison of the present analytical model with the one ignoring the initial stress induced by rotational centrifugal force, the present model is more accurate for the modeling consideration while the model ignoring the initial stress is a relative safe one for the engineering design consideration.

ACKNOWLEDGEMENTS

This research was supported by the following funding agencies: Ministry of Science and Technology, Taiwan (grant number MOST 107-2622-E-197-007-CC2); National Nature Science Foundation of China (grant number 11502227); and Shandong Provincial Natural Science Foundation, China (grant number ZR2018MEE021).

REFERENCES

Ayazi, F., Chen, H.H., Kocer, F., He, G., Najafi, K., “A High Aspect-Ratio Polysilicon Vibrating Ring Gyroscope,” Proceedings of the Solid-State Sensor and Actuator Workshop, Hilton Head Island, South Carolina, 4-8 June, 2000, 289-292.

Beli, D., Silva, P.B., Arruda, J. R. de F., “Vibration Analysis of Flexible Rotating Rings Using a Spectral Element Formulation,” ASME Journal of Vibration and Acoustics, 137, 041003-1–041003-11 (2015).

Cooley, C.G., Parker, R.G., “Vibration of High-speed Rotating Rings Coupled to Space-fixed Stiffnesses,” Journal of Sound and Vibration, 333, 2631–2648 (2014).

Chuang, W.C., Lee, H.L., Chang, P.Z., Hu, Y.C., “Review on the Modeling of Electrostatic MEMS,” Sensors, 10, 6149–6171 (2010).

Esmaeili, M., Durali, M., Jalili, N., “Ring Microgyroscope Modeling and Performance Evaluation,” Journal of Vibration and Control, 12, 537–553 (2006).

Huang, D., Tang, L., Cao, R., “Free Vibration Analysis of Planar Rotating Rings by Wave Propagation,” Journal of Sound and Vibration, 332, 4979–4997 (2013).

Huang, D., Tang, L., Cao, R., He, H., “Vibration Analysis of a Multi-Span Rotating Ring,” Proceedings of the 21st International Congress on Sound and Vibration, Beijing, China, 13-17 July, 2014.

Huang, S.C., Soedel, W., “Effects of Coriolis Acceleration on the Free and Forced In-plane Vibrations of Rotating Rings on Elastic Foundation,” Journal of Sound and Vibration, 115, 253–274 (1987).

Huang, S.C., Soedel, W., “Response of Rotating Rings to Harmonic and Periodic Loading and Comparison with the Inverted Problem,” Journal of Sound and Vibration, 118, 253–270 (1987).

Hu, Y.C., “Closed Form Solutions for the Pull-in Voltage of Micro Curled Beams Subjected to Electrostatic Loads,” Journal of Micromechanics and Microengineering, 16, 648–655 (2006).

Hu, Y.C., Chang, C.M., Huang, S.C., “Some Design Considerations on the Electrostatically Actuated Microstructures,” Sensors and Actuators A: Physical, 112, 155–161 (2004).

Kim, W., Chung, J., “Free Non-linear Vibration of a Rotating Thin Ring with the In-plane and Out-of-plane Motion,” Journal of Sound and Vibration, 258, 167–178 (2002).

Li, Y., Yu, T., Hu, Y.C., “The Stiffness Variation of a Micro-Ring Driven by a Traveling Piecewise-Electrode,” Sensors, 14, 17256–17274 (2014).

Meirovitch, L., “Analytical Methods in Vibrations,” Macmillan: New York, USA, 1967; ISBN: 0-0238-0140-9.

Soedel, W., Vibrations of Shell and Plates, 3rd ed.; Marcel Dekker, Inc.: New York, USA, 415–437(2005). ISBN: 0-8247-5629-0.

Tao, Y., Wu, X., Xiao, D., Wu, Y., Cui, H., Xi, X., Zhu, B., “Design, Analysis and Experiment of a Novel Ring Vibratory Gyroscope,” Sensors and Actuators A: Physical, 168, 286–299 (2011).

Ye, X., Chen, Y., Chen, D.C., Huang, K.Y., Hu, Y.C., “The Electromechanical Behavior of a Micro-ring Driven by Traveling Electrostatic Force,” Sensors, 12, 1170–1180 (2012).

Yu, T., Kou, J.; Hu, Y.C., “Vibration of a Rotating Micro-Ring Under Electrical Field Based on Inextensible Approximation,” Sensors, 18, 2044 (2018).

旋轉環於靜電場下的振動

于涛　寇建阁
烟台大学机电汽车工程学院
胡毓忠
國立宜蘭大學機械與機電工程學系

摘 要

因其應用廣泛，旋轉環頗受矚目，例如：振動環陀螺儀。本文提出一個旋轉環在均勻電場作用下之振動的解析模型。在分析旋轉環的振動之前，先推導出靜止環在靜電場作用下的靜態吸附電壓。然後推導出線性化的靜電場模型。當電壓小於靜態吸附電壓時，該線性化的靜電場模型與非線性模型相當吻合。因此，在分析旋轉環於靜態吸附之前的振動和穩定性時，則沿用該線性化的靜電場模型。靜電場會對旋轉環產生一個正比於電壓平方的等效負勁度，該等效負勁度會軟化環結構進而可能造成旋轉環的振動呈不穩定。最特別的是，當電壓值達到產生不穩定振動的範圍時，藉由增加環的轉速至超過所謂的臨界轉速，可使的旋轉環離開不穩區。此乃因離心力對環所造成的初始應力正比於轉速的平方，而該初始應力則可強化環的剛性。